ISBN: 978-3-95450-247-9 ISSN: 2673-5490 doi: 10.18429/JACoW-IPAC2024-TUPR76

EXPLORING CONVECTIVE HEAT TRANSFER COEFFICIENTS IN FULLY DEVELOPED FLOWS: A COMBINED CFD ANALYSIS AND EXPERIMENTAL VALIDATION FOR COMMON GEOMETRIES IN PARTICLE ACCELERATORS

J. Vàzquez i Mas*, G. Raush, R. Capdevila, Polytechnic University of Catalonia, Terrassa, Spain
J. Casas, C. Colldelram, M. Quispe, M. Sanchez
ALBA-CELLS Synchrotron, Cerdanyola del Vallès, Spain
G. Campolina, La Romanica School, Barberà del Vallès, Spain

Abstract

Within the field of Particle Accelerators engineering, the design of cooling channels for its components has heavily relied on experimental correlations to compute convective heat transfer coefficients. These coefficients are believed to have a conservative factor which end up in oversized designs.

The following study assesses this conservative factor for fully developed flows, in the laminar, turbulent and transition regimes. It will also focus on different geometries to do so. With this objective in mind, simulation models have been developed and correlated with experiments carried out at ALBA synchrotron. In the course of this research, various turbulence models and meshes have been examined for the development of the simulations. Heat transfer coefficients were derived from the Computational Fluid Dynamics (CFD) simulations and juxtaposed with empirical correlations. The specific geometries under investigation encompass a circular channel with a 10mm inner diameter, a rectangular section channel, and a pinhole geometry, the latter being frequently employed in Accelerator technology.

INTRODUCTION

Heat transfer for modern cooling system designs is studied with experimental correlations [1–3]. For circular sections the most used to calculate the Nusselt Number (Nu) (between $2300 \leq Reynolds\ (Re) \leq 5 \cdot 10^6$) are from Dittus & Boelter (Eq. (1)), Petuhkov (Eq. (2)) and Gnielinski (Eq. (3)):

$$Nu = 0.024 Re^{0.8} Pr^{0.4} \tag{1}$$

$$Nu = \frac{(f/2) Re\ Pr}{1.07 + \frac{900}{Re} - \frac{0.63}{1+10Pr} + 12.7\left(\frac{f}{2}\right)^{0.5}(Pr^{2/3} - 1)} \tag{2}$$

$$Nu = \frac{(f/2)(Re - 1000)Pr}{1 + 12.7(f/2)^{0.5}(Pr^{2/3} - 1)}, \tag{3}$$

where Pr is the Prandt number and f the friction factor. For rectangular sections these same equations are used applying the hydraulic diameter correction for the charecteristic length of the Reynolds number. For crotch absorber geometries, widely used in particle accelerators, experimental results are also used [4]. Prior studies from Refs. [5] and [6] show a 14% difference in Nusselt number between CFD and correlations in circular section tubes. This difference will be assessed again with an improved CFD model. Experimental validation will be also carried out to assess CFD accuracy.

* jordivzm@gmail.com

GEOMETRIES

Three different geometries have been studied during the research: a circular section steel pipe, a square section copper pipe (Fig. 1), and a copper *pinhole* geometry (Fig. 2). The latter is composed of two concentric circular pipes with a helicoid between them to boost heat transfer. Water enters through the inner pipe, and returns through the outer one.

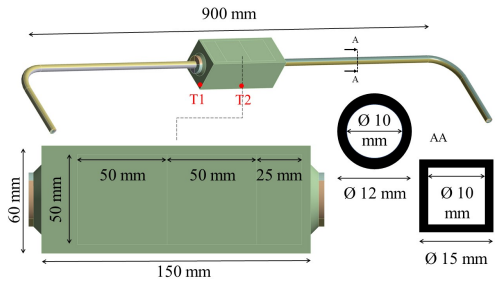

Figure 1: Mirror geometry with circular and square sections.

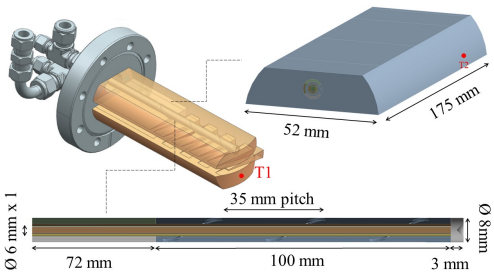

Figure 2: Pinhole geometry.

An experimental and CFD model of each geometry has been made. The experimental models aim to validate the reliability of the CFD model comparing the values of the temperatures at T1 and T2. Once this reliability has been verified CFD models are used to obtain the heat coefficients $\left(h = q/(T_w - T_f)\right)$ which are compared with the results of equations (Eqs. (1–3)). T_w is the wall temperature and T_f represents the fluid temperature. This comparison is made transforming h to Nu with: $Nu = hL/\lambda$.

ISBN: 978-3-95450-247-9 ISSN: 2673-5490 doi: 10.18429/JACoW-IPAC2024-TUPR76

CFD MODEL

General Set-up and Boundary Conditions

Even though geometries and meshes are different for each case there are common variables for all the simulations. For instance, water properties for dynamic viscosity, density, specific heat and thermal conductivy depend on the temperature of the fluid and are the same for all simulations. As boundary conditions, the velocity of the fluid will be set for each case while the heat flux will be fixed with a value of 10,880 W/m^2, resulting in 86.4 W. RANS Simulations will be made with Ansys Fluent, with the SIMPLEC algorithm.

The turbulence model is also the same for all simulations, chosen with a prior turbulence model study. The study included the $k-\omega$ SST model, $Transition\ SST$, $Rk-\epsilon$ and $GEKO$ and it was made with the geometry of Fig. 1. The models have been chosen because of their extensive use in industrial fluid mechanics applications. As it can be seen in Fig. 3, $Transition\ SST$, $Rk-\epsilon$ EWT and $Rk-\epsilon$ $ScWF$ have erratic behaviours probably because an incorrect prediction of the level of turbulence and an inadequate level of mixing of the fluid itself [7]. Because of its robustness and accuracy the $k-\omega$ SST model has been chosen to be used for the research [8].

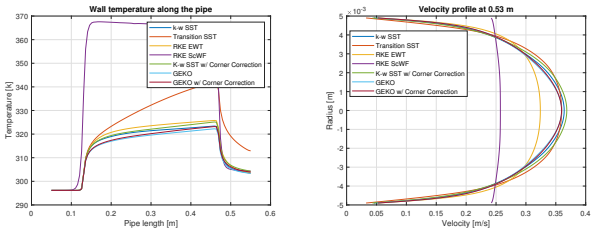

Figure 3: Turbulence model study variables

Meshing

A grid convergence study has been conducted for each geometry in order to have solutions independent from the mesh. For the geometry in Fig. 1 a structured mesh for the pipe was chosen and a $y^+ < 1$ reached [9]. However, due to the complexity of the pinhole geometry, it was simulated with a $y^+ > 30$ using standard wall functions.

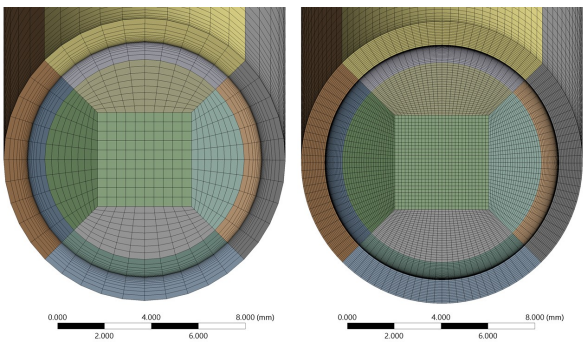

Figure 4: Coarse and fine mesh

EXPERIMENTAL MODEL

A closed system set-up similar to Rabasa's [6] was used for this research with two main innovations (see Fig. 5). Firstly, a chiller was used in the experiment which mantained inlet water stable at 23 ºC. Secondly, the geometry has been studied inside a vacuum chamer in order to eliminate natural convection to atmospheric air. There were two pumps connected to it that reached up to 10^{-5} mbar.

To recreate the effect of synchrotron radiation a constant heat flux is applied to the geometries using heater foils. Thermocouples type K were placed at different parts of the geometries (T1 and T2 in Figs. 1 and 2) to have comparation points with the CFD models. The water temperature was also measured at the inlet and outlet of the geometry. The outlet temperature is measured after a pipe corner in order to ensure sufficient level of mixing.

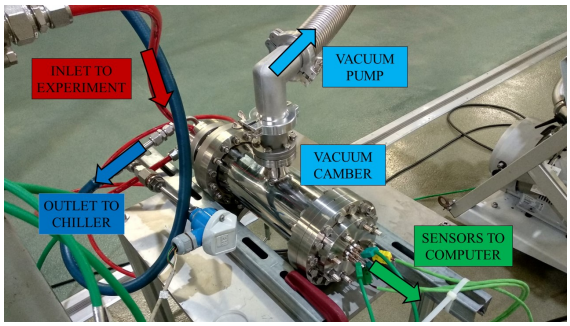

Figure 5: Experimental Set-up of the pinhole.

In Fig. 6 the temperature of the T1 sensor of the mirror geometry (see Fig. 1) is plotted for different massflows, as well as the temperature predicted by author correlations and CFD simulations. The temperatures of the authors are predicted with steady-state thermal Ansys simulations with a constant convection heat transfer coefficient.

The temperatures at T1 and T2 predicted by CFD and experiments have <5% difference once a turbulent regime is reached for both geometries of Figs. 1 and 2. Thus, the model for this regime is validated. However, at a laminar regime CFD seems to be innacurate.

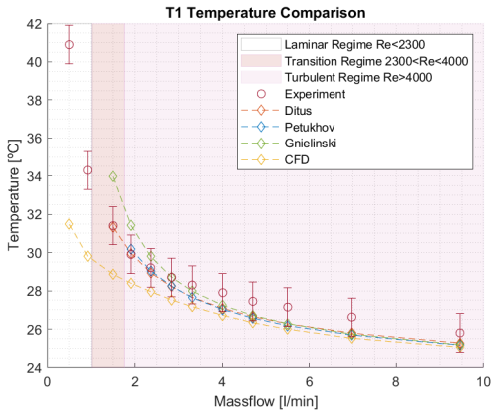

Figure 6: T1 of mirror geometry temperature comparison.

ISBN: 978-3-95450-247-9 ISSN: 2673-5490 doi: 10.18429/JACoW-IPAC2024-TUPR76

RESULTS

Mirror Geometry

Once the CFD model is validated the heat transfer coefficient prediction between CFD simulations and literature correlations can be compared for different flow regimes.

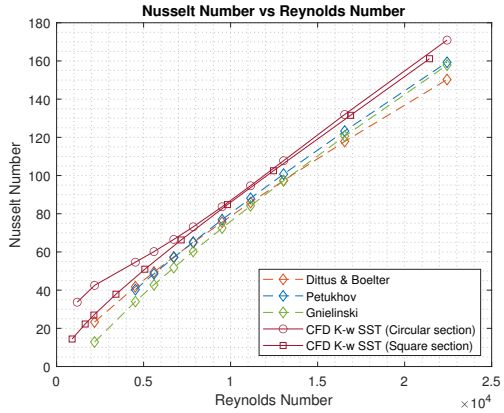

Figure 7: Nusselt predictions for the mirror geometry.

In Fig. 7 a slight difference in Nusselt number prediction between CFD and literaure correlations is observed. The difference varies for each author and Reynolds number, but it stabilizes at a high turbulent flow regime ($1 \cdot 10^4 < Re$) between 6.5% and 12% (see Table 1). At lower Reynolds there is a discrepency in the Nusselt prediction probably caused because of the extra turbulence generated by the inlet corner of the mirror geometry, which increases the Nusselt number in CFD simulations. The square section simulations did not have the inlet corner and do not show this increment in Nusselt prediction.

Table 1: Nusselt Number Difference Between CFD and Literature Correlations in % in Circular Section.

Reynolds	**4,53E+03**	**7,85E+03**	**1,11E+04**	**1,66E+04**
Dittus	23.5%	11.3%	9,3%	10.7%
Petukhov	26.3%	10.9%	6.9%	6.6%
Gnielinski	37.7%	17.6%	11.1%	8.6%

Pinhole Geometry

The results of the pinhole analysis have been contrasted to Swiss Light Source (SLS) synchrotron experimental data [10] and Grozavu's paper [5] due to the lack of literature regarding this type of geometry (see Fig. 8). CFD presents the same tendency as the experimental results, with a slight offset (1.5% - 8%) at the turbulent regime (see Table 2).

Table 2: Heat Transfer Coefficient Difference Between CFD and Experimental Correlation in % in Pinhole.

Massflow [gr/s]	**16.7**	**28.3**	**41.7**	**55.0**	**91.7**
Error	-1.6%	8.0%	6.8%	5.7%	7.2%

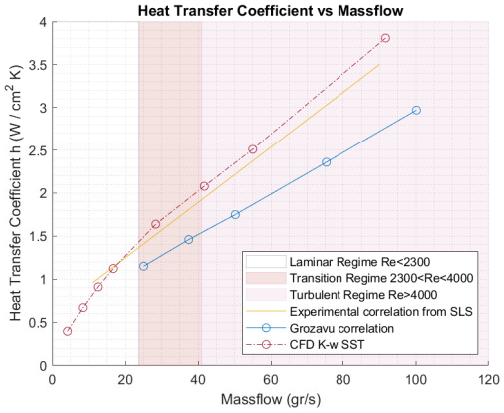

Figure 8: HTC predictions for the pinhole geometry.

Figure 9 shows that the temperatures are not constant at the geometry, so the heat transfer coefficient will not be constant either. The final coefficient is calculated as an average throughout the pipe. The main heat transfer has been found to be at the exterior pipe, where the helicoid is.

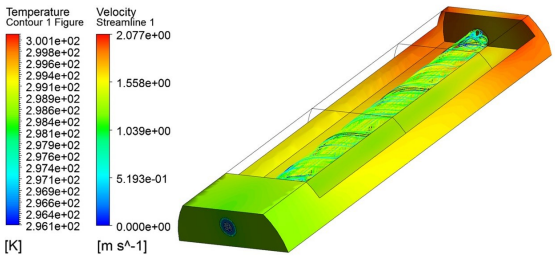

Figure 9: Temperature and velocity map (1l/min massflow).

CONCLUSION

Research on heat transfer convective coefficient has been conducted on common geometries in particle accelerators cooling systems technologies. CFD analysis, which has been validated with experimental results (see Fig. 6), shows the same tendency as experimental correlations for all the geometries. However, CFD overpredicts the Nusselt number in circle and square sections by 6.5% - 12% in turbulent regime when compared to author correlations (see Fig. 7). The same behaviour is observed for the pinhole geometry, with an error of 1.5% - 8% (see Fig. 8).

With this study an oversizing of the designs made directly with literature correlations is observed. The technical and environmental implications of this are highly favorable, as reduced fluid flow requirements would effectively dissipate the same heat, leading to less power requirements and resource consumption, less vibrations and extended component lifespan. Furthermore, CFD is able to depict the local behaviour of the heat transfer coefficient, whereas designs with literature correlations are unable to analyse this detail.

ISBN: 978-3-95450-247-9 ISSN: 2673-5490 doi: 10.18429/JACoW-IPAC2024-TUPR76

REFERENCES

[1] F. W. Dittus and L. M. K. Boelter, "Heat transfer in automobile radiators of the tubular type", in *University of California Publications in Engineering*, 1930, vol. 2, pp. 443–461.

[2] B. S. Petukhov, "Heat Transfer and Friction in Turbulent Pipe Flow with Variable Physical Properties", in *Advances in Heat Transfer*, 1970, vol. 6, pp. 503–564.

[3] V. Gnielinski, "Neue Gleichen für den Wärme und den Stoffübergang in turbulent durchströmten Rohren und Kanälen", *Forsch. Ingenieurwes.*, vol. 41, pp. 8–16, 1975.

[4] M. Quispe, E. Al-Dmour, E. Dieter,R. Martin, L. Nikitina, and R. Llibert, "Development of the Crotch Absorbers for ALBA Storage Ring", in *Proc. MEDSI'08*, 2008, pp. 1–-15.

[5] S. Grozavu, J. J. Casas, C. Colldelram, M. Quispe, and G. A. Raush, "CFD Studies of the Convective Heat Transfer Coefficients and Pressure Drops in Geometries Applied to Water Cooling Channels of the Crotch Absorbers of ALBA Synchrotron Light Source", in *Proc. IPAC'22*, Bangkok, Thailand, Jun. 2022, pp. 2887–2890. doi:10.18429/JACoW-IPAC2022-THPOTK050

[6] M. Rabasa *et al.*, "CFD studies and experimental validation of the convective heat transfer coefficient in non-fully developed flows applied to conventional geometries used in particle accelerators", in *Proc. IPAC'23*, Venice, Italy, May 2023. doi:10.18429/JACoW-IPAC2023-THPM010

[7] M. Kadivar, D. Tormey, and G. McGranaghan, "A comparison of RANS models used for CFD prediction of turbulent flow and heat transfer in rough and smooth channels", *Int. J. Thermofluids*, vol. 20, p. 100399, 2023.

[8] F. R. Menter, R. Lechner, and A. Matyushenko, "Best Practice: RANS Turbulence Modeling in Ansys CFD", Technical Paper, Ansys, 2021.

[9] LEAP CFD Australia, "Understanding the physics of boundary layers", 2020. https://www.computationalfluiddynamics.com.au/y-plus_part1_understanding-the-physics-of-boundary-layers

[10] G. Heidenreich, L. Schulz, and A. Matyushenko, private communication, Paul Scherrer Institute. 2007